Title : will be set by the publisher
Editors : will be set by the publisher
EAS Publications Series, Vol. ?, 2010

OSCILLATOR STENGTHS AND THEIR UNCERTAINTIES

Glenn M. Wahlgren[1, 2]

Abstract. The oscillator strength is a key parameter in the description of the line absorption coefficient. It can be determined through experiment, *ab initio* and semi-empirical calculations, and backward analysis of line profiles. Each method has its advantages, and the uncertainty attached to its determination can range from low to indeterminable. For analysis of line profiles or equivalent widths the uncertainty in the oscillator strength can rival or surpass the difference between the derived element abundance from classical LTE and non-LTE analyses. It is therefore important to understand the nature of oscillator strength uncertainties and to assess whether this uncertainty can be a factor in choosing to initiate a non-LTE analysis or in the interpretation of its results. Methods for the determination of the oscillator strength are presented, prioritizing experiments, along with commentary about the sources and impact of the uncertainties. The Se I spectrum is used to illustrate how gf-values can be constructed from published data on atomic lifetimes and line intensities.

1 Introduction

The oscillator strength, or f-value, is one measure of the strength of a spectral transition. It can be determined from experiment, theory, or analysis of spectral lines when other parameters are known. The uncertainty in the f-value ranges from levels of a few percent, for tractable experiments, to very poor, and in some cases it is indeterminable. The f-value and its uncertainty play key roles in line profile analysis and in determining the relative merit of different analysis paradigms.

It has long been appreciated by spectroscopists that the physical conditions of a light-source plasma can comprise non-local thermodynamic equilibrium (non-LTE) processes, and as a result, influence the interpretation of the analysis and

---

[1] Dept. of Physics, Catholic University of America, 620 Michigan Ave NE, Washington DC 20064, USA

[2] NASA Goddard Space Flight Center, Code 667, Greenbelt, MD 20771, USA; e-mail: `Glenn.M.Wahlgren@nasa.gov`

DOI: (will be inserted later)

the uncertainties. It was expressed by Blackwell (1990) that "... a vital part of the determination of an oscillator strength is the assessment of a probable error. If this is not done reliably, for example, an apparent detection of non-LTE in a stellar atmosphere might only be due to errors in the adopted oscillator strengths."

To elucidate this last point, let us consider the influence of the f-value uncertainty on LTE and non-LTE analyses of a stellar spectrum. For this exercise it is assumed that the atmospheric structure is essentially the same for both formalisms. We express the equivalent width, W_λ, of a weak absorption line (linear portion of the curve of growth) of a trace element as

$$W_\lambda \propto n_i f_{ij} \lambda_{ij}^2 \,, \tag{1.1}$$

where for a transition between lower energy level i and upper level j, n_i is the number density for the atom in level i, f_{ij} is the oscillator strength, and λ_{ij} is the transition wavelength. Equation 1.1 can be rearranged as an expression for the number density in level i

$$n_i \propto \frac{W_\lambda}{\lambda_{ij}^2 f_{ij}} . \tag{1.2}$$

The quantities W_λ and λ_{ij} can be measured to high accuracy from high quality stellar and laboratory spectra, respectively, and can have negligible uncertainty. Therefore, the uncertainty in n_i is proportional to the uncertainty in f_{ij}.

$$\delta n_i \propto \frac{W_\lambda}{\lambda_{ij}^2 f_{ij}^2} \delta f_{ij} \tag{1.3}$$

By definition, the ratio of the population for energy level i in non-LTE and LTE is parameterized by the departure coefficient, b_i,

$$b_i = \frac{n_{non-LTE}}{n_{LTE}} \,. \tag{1.4}$$

The departure coefficient is a measure of the deviation of the level population from that determined from the Saha and Boltzmann formulae (see Kubát and Mashonkina, this volume), and it has a value of unity when particle collisions are sufficent in number to establish LTE. For small (and perhaps not small) deviations from LTE, the difference between non-LTE and LTE number density can be equated to the uncertainty in f by claiming that the difference in n_i is an error (or uncertainty) in the LTE analysis.

$$\Delta n = n_{non-LTE} - n_{LTE} = n_{LTE}(b_i - 1) \,. \tag{1.5}$$

The percentage error in n_i with respect to the LTE analysis is

$$\frac{\Delta n}{n_{LTE}} = |b_i - 1| \propto \frac{\delta f_{ij}}{f_{ij}} = \frac{\delta n_i}{n_i} \,. \tag{1.6}$$

One can refer to diagrams that present b_i as a function of optical depth for individual energy levels (for example, see Fig. 1 of Mashonkina (this volume)) to make the comparison expressed by Eq. 1.6. This simple comparison can aid in evaluating whether the available f-values are accurate enough for claiming that the non-LTE analysis provides more meaningful results than a LTE analysis for a given spectral line. One must therefore consider the energy levels, the region of line formation in the stellar atmosphere (optical depth, τ), and the uncertainty in f, when assessing whether oscillator strengths are a limiting factor in a non-LTE interpretation.

The following discussion provides a brief overview of the oscillator strength and its uncertainty with the aim of providing considerations for analyzing stellar spectra. We concentrate on the experimental determination of f-values and their uncertainties. Calculated f-values and astrophysical gf-values are briefly discussed, but their uncertainties are of a different nature compared with those of experiment.

2 Basics of oscillator strengths

The oscillator strength has its origins in the classical approach to determining the index of refraction (n) in a dispersive medium, given the presence of an electric field. Invoking arguments of polarizability, Eq. 2.1 is derived. In the general sense, the quantity f_s in Eq. 2.1 is the number of oscillators of species s having a frequency of oscillation ω_s for a unit volume containing N molecules (see Ditchburn 1963 for derivation).

$$\frac{n^2-1}{n^2+2} = \frac{4\pi}{3}\frac{Ne^2}{m}\sum_s \frac{f_s}{\omega_s^2-\omega^2+i\gamma_s\omega} \tag{2.1}$$

Solving for the real part of the index of refraction leads to the well-known dispersion relation (Mihalas 1978, Parkinson 1987, Thorne, Litzén & Johansson 1999, among others)

$$n-1 = \frac{e^2N_if_{ij}}{2\pi m}\frac{\nu_{ij}^2-\nu^2}{(\nu_{ij}^2-\nu^2)^2+(\gamma\nu/(2\pi))^2}\,. \tag{2.2}$$

The reader is cautioned that the derivation of Eq. 2.2 can be presented in different forms.

In the quantum mechanical view of the interaction between radiation and matter, a photon of frequency ν is absorbed by an atom to cause a transition between two electronic states having an oscillator strength f_{ij}. Since the absorption coefficient (see Sect. 2.1) can be expressed in terms of the Einstein coefficients, the dimensionless Ladenburg f-value (Ladenburg 1921, 1928, 1933) is derived to be

$$f = \frac{g_j}{g_i}\frac{\epsilon_o m_e c^3}{2\pi e^2\nu^2}A_{ji}\,, \tag{2.3}$$

where A_{ji} is the Einstein transition rate for spontaneous decay. In this depiction the f-value can also be interpreted as the fraction of valence electrons that are likely to participate in the transition.

Although the f-value is an indicator of line strength, it is often presented weighted by the statistical weight, g, of the level from which the transition originates. The gf-value is therefore expected to be larger when: a) there are fewer decay channels, thus funneling the decay into fewer possible channels (only one channel in the case of ground state resonance lines), and/or b) the number of sublevels increases ($g_J = 2J + 1$ in the general case, or $g_n = 2n^2$ for hydrogenic ions). An increase in the number of sublevels is a natural consequence of increasingly higher energy states. However, that increase in the number of sublevels is often offset by the increased number of possible decay channels. The highest values for gf are typically between 10 and 100, regardless of where the levels are located in the energy system of an atom or ion. This is evident from the entries in the atomic data base of Kurucz (1993), for which only 535 lines have $\log(gf)$ between 1.0 and 2.0, and only a single line has a value (slightly) in excess of 2.0.

Transitions having large gf-values do not necessarily produce strong, observable spectral lines. Local conditions of the plasma, characterized by the temperature, pressure and chemical composition, play a strong role in the total absorption or emission for a specific transition. For cases where non-LTE is important, the observed intensity of a spectral line is influenced by distant (non-local) plasma conditions and radiation field.

2.1 Relationships between f, A, κ

A beneficial situation for determining atomic data is the redundancy that exists in expressing certain parameters that are used to describe radiative transitions. These relationships link theoretical quantities with observables, coupling atoms to radiation. For an atom in the presence of a radiation field (energy density), the Einstein coefficients for spontaneous decay, A_{ji}, stimulated absorption, B_{ij}, and stimulated emission, B_{ji}, are inter-related through the expressions

$$A_{ji} = \frac{8\pi h\nu_{ji}^3}{c^3} B_{ji}\,, \tag{2.4}$$

$$\frac{B_{ji}}{B_{ij}} = \frac{g_i}{g_j}\,. \tag{2.5}$$

These relations are valid under conditions of LTE and non-LTE, since they are properties of the atom alone and not the plasma conditions. The independent determination of one of these coefficients will allow for the determination of all three through the above relations. As it is typical to measure A_{ji} from the laboratory experiments mentioned in Sect. 3.1, both B_{ij} and B_{ji} can subsequently be calculated.

In addition to radiation processes, the effect of collisions can be included in the equations of detailed balance. The use of collisional excitation rate coefficients, C_{ij}, and their product with the number density of particles in level i, produces expressions for the total number of collisions, n_iC_{ij}. (See Kubát in this volume for discussion of the inclusion and effects of collisions on rate equations.) The improper treatment of collisions, i.e., their neglect when needed, therefore becomes a source of uncertainty in the solution of the rate equations and derived abundances.

To get a firmer understanding of the role of the f-value in spectral line calculations we start by expressing the *residual intensity* as the ratio of the frequency dependent intensity, I_ν, relative to the local continuum level, $I_{\nu o}$, which is a measureable quantity, in terms of the optical depth, τ_ν, and an effective mass absorption coefficient, $\kappa_\nu \rho$,

$$\frac{I_\nu}{I_{\nu o}} = \exp(-\tau_\nu) = \exp(-\kappa_\nu \rho \Delta x), \tag{2.6}$$

where κ_ν is the absorption coefficient, ρ is the mass density, and Δx is a measure of distance over which the absorption occurs. Equation 2.6 is one form of the solution of the equation of radiative transfer (see L. Chevallier and J. Kubát in this volume for solving the transfer equation), and the integration of (1- $I_\nu/I_{\nu o}$) over all frequencies defines the line equivalent width.

The optical depth can be expressed in terms of the sum of the line absorption coefficient, $\kappa_{\nu l}$, and the continuum absorption coefficient, $\kappa_{\nu c}$,

$$d\tau_\nu = (\kappa_{\nu l} + \kappa_{\nu c})\rho dx. \tag{2.7}$$

The coefficient $\kappa_{\nu c}$ is the sum of the frequency-dependent absorption coefficients from all bound-free and free-free processes and represents a slowly varying function relative to spectral line profiles. The coefficient for bound-bound processes, $\kappa_{l\nu}$, represents a rapid variation in the absorption coefficient, and can be expressed as

$$\kappa_{\nu l} = \frac{N}{\rho}\alpha_\nu = \frac{N}{\rho} C f V\,, \tag{2.8}$$

where N is the number density of the element under consideration, α_ν is the atomic absorption coefficient, V is the Voigt profile, C is the product of constants and f is the oscillator strength. Integration of α_ν over all frequencies

$$\int \alpha_\nu d\nu = (\pi e^2/m_e c) f \tag{2.9}$$

provides the dependence on f. Therefore the uncertainty in the f-value is transferred into an uncertainty of the atomic absorption coefficient. It is of interest to note that the continuum absorption coefficient also contains an oscillator strength, assuming the transition to occur between a bound energy state and a bound state in the continuum. This continuum f-value is computed by a simple expression, which also has an uncertainty that is incorporated into the continuum computation.

From these expressions it is evident that: 1) the f-value can be derived from direct measurement of the line profile and knowledge of certain parameters, and 2) redundant information associated with f-values and absorption coefficients can exist. The redundant information can be used to test f-values derived from different sources. The Einstein coefficient B_{ij} is related to κ_ν through

$$\frac{dB_{ij}}{d\nu} = \frac{c}{n_i h \nu_{ij}} \kappa_\nu \,. \tag{2.10}$$

It can be determined from experiments utilizing an absorption line spectrum. However, this requires accurate values of the temperature to compute particle densities for the gas through application of the Boltzmann equation. The uncertainty in measuring these parameters can be formidable.

2.2 Natural line broadening

An important and often overlooked benefit to accurately determining f by experiment or calculation is the ability to compute the natural broadening constant for a line having known level lifetimes. Natural line broadening arises from the uncertainty in the energies of electronic states, in effect an application of the Heisenberg uncertainty principle. It can be parameterized by a damping constant (Thorne, Litzén, & Johansson 1999)

$$\delta\nu_{ji} = (2\pi\tau_j)^{-1} + (2\pi\tau_i)^{-1} \,, \tag{2.11}$$

where it is clear that the broadening is dependent on the lifetimes (τ) of both energy levels. Since the ground state lifetime is infinitely long, transitions involving the ground state only need to consider the lifetime of the upper level. For resonance lines, starting from an accurate f-value, one can use equations presented in Sect. 3.1 to work backwards to derive the atomic lifetime of the upper level. For non-resonance lines, where both lifetimes are needed in Eq. 2.11, a scheme may need to be developed, starting with resonance lines or lines having known lifetimes, in order to derive lifetimes that are unknown. It is common for synthetic spectrum codes to compute natural line broadening parameters from a frequency-dependent algorithm, such as Eq. 2.12, thus ignoring the energy level lifetimes.

$$\gamma_{classical} = \frac{2\pi e^2 \nu_0^2}{3\epsilon_o m_e c^3} \tag{2.12}$$

For transitions allowed by the selection rules of quantum mechanics (spin and parity allowed), energy levels typically have lifetimes of order 10^{-8} s. In this case, the error, or difference, between the frequency approach (Eq. 2.12) and the use of lifetimes (Eq. 2.11) is small. However, for allowed transitions of longer lifetime, along with semi-forbidden (10^{-6} s $< \tau < 10^{-3}$ s) and forbidden transitions ($\tau > 10^{-3}$ s), the use of Eq. 2.12 leads to larger errors in computed natural broadening and possibly the derived element abundance. Synthetic spectrum fitting will be affected, since the line width and depth will not be well-fitted simultaneously. Wahlgren et al. (2001) provide an example of the problems with damping constants based on analysis of Bi II in a warm star. In summary, the application of the mean lifetime of energy levels can improve the accuracy of the line absorption coefficient through both line broadening and the f-value. Although the number of measured lifetimes is relatively small compared with the total number of lines in a synthetic spectrum analysis, they are most often available for resonance lines and lines of low excitation energy, which are often used in stellar chemical abundance analyses.

3 Oscillator strengths from experiment

Experiments in absorption and emission spectroscopy have been developed for the determination of f-values. An experimental setup is comprised of a light source, a dispersive element and detector, along with the associated electronics and data recording device. Each component of the experiment contributes to the uncertainty of the results. In addition to their utility for analysis of astronomical spectra, the accurate determination of oscillator strengths through measurement provides fundamental atomic data that can be used to test atomic structure theory.

3.1 Construction of the oscillator strength

We discuss the determination of the oscillator strength from the perspective of emission line spectroscopy, i.e. populating an excited level and measuring the subsequent radiation emitted upon its decay. With time-dependent experiments, one has the capability to measure the rate of decay of the upper-level population. Therefore, both the spectral line intensities and level lifetimes can be measured. Absorption or emission lines can be used to measure relative f-values. If the conditions of the plasma (temperature and density) can be determined, then accurate relative f-values may be derived from absorption lines (Blackwell & Collins 1972). A conversion between emission and absorption oscillator strengths can be accomplished through application of the relation

$$f_{ij} = -\frac{g_j}{g_i} f_{ji}\,. \tag{3.1}$$

The intensity of an emission line in energy units, corrected for instrumental effects, is given by the relation

$$I_{ji} = N_j h\nu_{ji} A_{ji}\,, \tag{3.2}$$

which shows it to be proportional to the total population of the transition's upper level, N_j, the frequency of the transition, ν_{ji}, and the transition rate for spontaneous decay, A_{ji}. The upper level may have several decay channels, which will lead to the creation of an equivalent number of emission lines whose relative intensities are proportional to the product of their transition probabilities and frequencies. Using Eq. 3.2, we define the branching fraction, BF, as the ratio of the intensity of the line of interest relative to the combined intensity of all emission lines originating from that same upper level, which in terms of frequencies is given by,

$$(BF)_{ji} = \frac{I_{ji}}{\Sigma_k I_{jk}} = \frac{A_{ji}\nu_{ji}}{\Sigma_k A_{jk}\nu_{jk}}. \tag{3.3}$$

Equation 3.3 can be expressed in terms of wavelengths as,

$$(BF)_{ji} = \frac{I_{ji}\lambda_{ji}}{\Sigma_k I_{jk}\lambda_{jk}} = \frac{A_{ji}}{\Sigma_k A_{jk}}. \tag{3.4}$$

The mean lifetime, τ_j, of the excited level j is related to the transition probabilities for all emission lines to levels $i < j$,

$$\tau_j = \frac{1}{\Sigma_i A_{ji}}\,. \tag{3.5}$$

τ_j is the time constant in the expression for the decay of level j for emission line intensity,

$$I_{ji}(t) = A_{ji} h\nu_{ji} N_j(t=0) \exp(-t/\tau_j)\,. \tag{3.6}$$

Since the frequencies of the multiplet transitions tend to be close in value, we often write the transition probability for the line of interest in terms of the branching fraction and the mean lifetime,

$$A_{ji} = \frac{(BF)_{ji}}{\tau_j}\,. \tag{3.7}$$

Finally, the dimensionless f-value can be related to the transition probability through the expression

$$f_{ji} = 1.499 \times 10^{-8} \frac{g_j}{g_i} \lambda^2 A_{ji}\,, \tag{3.8}$$

where the units are $\lambda(\text{Å})$ and $A(10^8\ \text{s}^{-1})$.

Using this approach, the results from one or two experiments will produce the necessary data (τ_j and I_{ji}) for determining the gf-value for a line. In practice, the uncertainties that result are dependent on the nature of the experiment, and it may be very difficult to reduce the uncertainties to a level that is required to address the scientific objectives.

3.2 Intensity measurements and branching fractions

Spectral line intensities can be measured using data obtained from a variety of laboratory spectrographs and spectrometers. Important factors for determining accurate atomic data include a high instrument resolving power, high signal-to-noise (S/N), extensive wavelength coverage, and the ability to perform accurate calibration of the wavelength (frequency, wavenumber) and intensity.

The wavelength coverage of the experiment should be extensive enough to record all lines originating from the same upper level, if possible. The intensity of all unobserved lines from the multiplet is referred to as the *residual* intensity. When the observations cannot include all lines of a multiplet, a theoretical approach or inference from astronomical spectra may be necessary to estimate the residual. The S/N of the spectrum should be high enough to accurately measure all lines of the multiplet to within the desired accuracy. Measurement errors influence the computation of the BF for each line and are transferred directly into uncertainties in A and f. The S/N of a line, and therefore its measurement uncertainty, may differ by orders of magnitude among lines from the same multiplet, which reflects their respective transition probabilities. Within a multiplet, the uncertainty in the gf-value of a weak line can be considerably higher than that for a strong line solely due to the laboratory intensity. This uncertainty from the line intensity is then combined with the uncertainty of the atomic lifetime, which is the same for all lines of the multiplet.

Figure 1 presents a segment of the selenium spectrum taken with the NIST 2 m FTS and a hollow-cathode discharge lamp (HCL) having selenium pellets in its cathode. The figure presents intensity in the form of S/N prior to intensity calibration and shows that the measurement of each peak should have an uncertainty of less than 1%. The BF for each line will also have this level of accuracy. The intensity calibration is performed by dividing the observed selenium spectrum (Fig. 1) with the sensitivity curve of the instrument setup (Fig. 2), which was obtained from an observation of an absolute flux calibrated quartz lamp. The high number of counts (high S/N) of the calibration spectrum will not be the limiting factor in the relative S/N among the Se I lines. The three lines of Se I multiplet 1 are found in close wavelength proximity and will have a similar uncertainty in their flux calibration.

An alternate method for intensity calibration is to create branching ratios, $BR = I_1/I_2$, the ratio of intensities for lines in close proximity to each other. It is common to use a number of line pairs from the carrier gas spectrum, typically argon and neon, which have previously been measured for their absolute intensity over a range in wavenumber. The spectrum intensity can then be adjusted according to the line pair sensitivity envelope.

The light source plasma need not be in thermodynamic equilibrium (TE) or local thermodynamic equilibrium (LTE) for the determination of BFs. Light sources such as the HCL are non-LTE plasmas, since energy levels are selectively excited by the carrier gas and do not follow Boltzmann statistics. However, since we determine f-values for the lines of a complete multiplet in this manner, i.e. all lines related through the same upper level and therefore the same lifetime, it is unimportant whether different multiplets are in equilibrium with each other according to Boltzmann statistics.

The excitation in a HCL is provided by inductive heating. Atoms of the carrier gas collide with the metal comprising the cathode and the element placed inside it to sputter out atoms that then become ionized and/or excited through collisions with carrier gas atoms and free electrons. The choice of carrier gas imposes limitations on the excitation imparted to the sputtered material. Nobel gases (He, Ne, Ar, Kr) are typically used as the carrier gas, with the heavier, and therefore slower, particles producing reduced levels of ionization and excitation compared with the use of the lighter, faster atoms. The use of a mixture of gases, such as He-Ne, often employs the heavier atom to create sputtered material and the lighter atom to impart a higher excitation to the sputtered atoms. The HCL is useful for

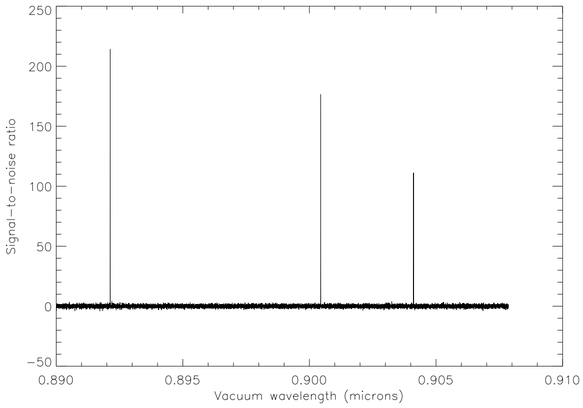

Fig. 1. The transitions $4p^3(^4S^o)5s^5S^o_2 - 4p^3(^4S^o)5p^5P_{1,2,3}$ in Se I (multiplet 1) prior to intensity calibration. Data were obtained using the NIST 2 m FTS.

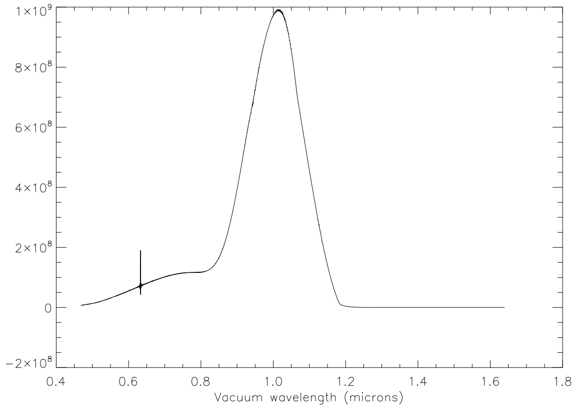

Fig. 2. Quartz lamp spectrum used for intensity calibration of spectrum in Fig 1. The spike at 0.63 μm results from the He-Ne laser that guides the FTS operation. The ordinate quantity is counts.

producing the spectrum of neutral and singly-ionized atoms, and perhaps doubly-ionized atoms if the ionization potential of the singly-ionized species is sufficiently low (e.g. lanthanide elements). To produce the spectrum of more highly excited species requires the use of other light sources, such as the Penning, spark, and sliding-spark discharge, and pulsed sources. The combination of instrument and light source can have limitations. For example, the Fourier transform spectrometer (FTS) is used with a temporally stable light source, which would not allow for it to be used with pulsed sources.

3.3 f-values determined directly from emission line intensity

Emission line intensities have been used to directly determine f-values. In this context, the work of Corliss & Bozman (CB, 1962) stands out as the prime historical example. Their work was originally intended to determine relative intensities of spectral lines for quantitative spectroscopic analysis. However, they realized that useful f-values could be derived from the measurements for application by astronomers to the new work being performed on determining the abundances of the chemical elements in stars. The chemical composition of the Sun was of particular interest at that time.

The CB data set comprised arc spectra photographed at five grating settings, covering the wavelength interval from 2000 Å to 9000 Å. The electrodes used in the experiments had a common composition ratio of element Z to copper of (Z:Cu) = (1:10000). Their procedure for determining f-values was of the following:

- measure line intensities, I, from high-quality laboratory spectra
- determine the *effective temperature*, T, of the arc source from measured I and *published* transition probabilities, A, or gf-values for lines of many elements by application of the Boltzmann equation (creation of a mean T)
- for many elements, measure the degree of ionization using the Saha ionization equation with measured I and *published* A, to determine the best (mean) value for electron density
- determine *relative* transition probabilities on a uniform scale for all classified lines
- place the uniform scale on a normalized absolute scale by comparison with *published* absolute A values for many different spectra.

The use of the terminology *effective temperature* by CB does not have the same meaning as in astronomy, where $T_{\rm eff}$ is associated with the Planck function. The CB effective temperature denotes a characteristic temperature of the arc source, as determined from the Boltzmann distribution. In this sense, the CB temperature can be considered the excitation temperature.

The result of their seminal study was a tabulation of gf-values for approximately 25 000 classified lines, covering 70 elements, which has proven to be an incredibly useful resource. However, it was quickly realized that the CB gf-values can have large, systematic errors, and that checks were needed for the absolute oscillator strength scale (Garstang 1968; Zwaan 1967). According to Parkinson (1971), in reference to the spectrum of Fe I, “As a result of the two shock tube absorption experiments we recognized that the ‘normalization function’ applied by Corliss and Bozeman in the free-burning arc for high excitation lines was incorrect, making their gf -values nearly an order of magnitude too high.”

Looking back with hindsight, one might expect large, possibly systematic uncertainties in the work of CB by their use of contemporary A values, which were an ecclectic set of data. Their use of average electron density, the assumption of a linear relationship to determine the source temperature, and the use of published gf or A values, which have their own uncertainties, form the basis of an averaging process for the creation of an absolute f-value scale. Cowley & Warner (1967), Cowley (1983), Cowley & Corliss (1983) and Bord, Barisciano & Cowley (1996) explored methods to correct the intensity scale of Meggers, Corliss, & Scribner (1975), which provided updated values of the original CB work for individual species. Attempts have also been made by R. Kurucz to make systematic ion-dependent corrections to the CB f-values using more recent data for common lines.

Laboratory studies typically do not yield measurements for a large number of lines or levels, or are restricted in wavelength. Therefore, not all spectral lines assigned gf-values by CB have been reanalyzed by modern techniques. There remain many lines in data bases that utilize the CB gf-values despite the fact that experimentally determined gf-values can be derived from published modern values of lifetimes and line intensities. The uncertainties for CB data can be large and systematic for an entire spectrum, but not for every element and not of the same magnitude. From experience, we note that, on average, the gf-values of CB are larger than the reanalyzed values. It is not unusual to find a gf-value in excess of unity in the CB data set, whereas updated gf-values present fewer lines of such strength. An error in the CB gf-values of a factor of 10 is not rare.

3.4 Experimental determination of lifetimes

Modern techniques for measuring atomic lifetimes involve populating excited levels of atoms/ions and recording their subsequent decay via observable emission lines. The decay curve is fitted with an exponential function(s) to determine the mean lifetime for upper level j, which is the time constant in the expression

$$I_{ji}(t) = I_{ji}(t=0)e^{-(t/\tau_j)} \,. \tag{3.9}$$

The lifetimes are then used to determine the transition rates, A_{ji}, and oscillator strengths, f_i. The basic difference among experimental techniques is the method employed to populate excited states, since for all of the techniques the lifetime is extracted from a radiative decay measurement. Excited states are populated by either selective or non-selective techniques, meaning, respectively, that specific energy levels are targeted for population or many levels are populated simultaneously. Selective excitation techniques involve the use of particle beams and lasers to study allowed transitions, and laser probing of storage-ring beams for measuring the longer lifetimes of forbidden transitions (Mannervik 2003).

An example of a two-laser system is that at the Lund Laser Centre, Lund University (Li et al. 1999). At this facility, laser-induced florescence (LIF) is created by directing a pulsed, ablation laser at a rotating metal target to produce a plasma cone. A second, pulsed laser interacts with the plasma cone to populate excited states according to the laser frequency. By recording the decay of a chosen spectral line with high-speed electronics, lifetimes as short as 1 ns can be

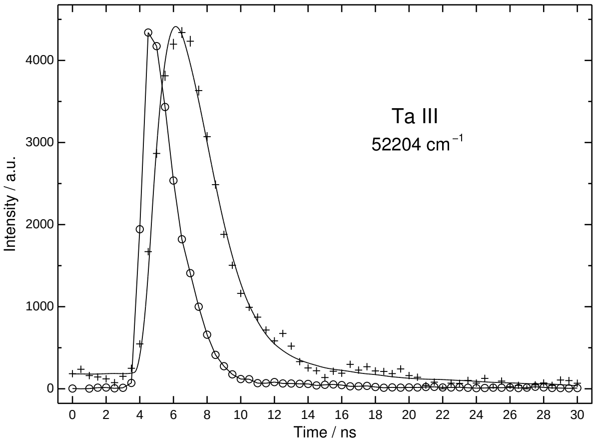

Fig. 3. Decay curve for the Ta III 5d^{2}6p(3/2)^o 52203.92 cm^{-1} energy level. Plus signs designate measurements of the Ta III line and open circles define the decay of the excitation laser pulse. Figure courtesy of L. Engström (Lund Laser Centre).

measured. The advantage of this system is in the selective nature of the excitation (narrow bandwidth), and the ability to measure lifetimes and line intensity with the same experiment, although the latter typically with lower accuracy than classical techniques utilizing dispersive gratings or Fourier transform spectroscopy. The problems inherent in this system include the limited lifetime range that can be measured (approximately 1 ns to 60 ns, in Lund) due to the physical size of the experiment, and the ability to work with only low ions for allowed states, due to currently usable laser dyes and laser energies. This is a time consuming process, since one needs to measure levels individually, and many repetitions of the experiment are conducted to obtain an adequate S/N for the decay curve. Figure 3 presents the decay curve observed from Ta III λ1915.565 Å compared with the decay curve of the excitation laser, which defines the shortest measureable lifetime. Fitting the slope of the decay curve determines the lifetime, which for both curves in Fig. 3 was determined to be 1.5 ± 0.2 ns (Fivet et al. 2008).

An example of a non-selective technique for measuring atomic lifetimes is beam-foil spectroscopy. It was pioneered in the 1960s (Kay 1963; Bashkin 1964; Martinson 1998) and it has provided lifetimes for many ions. For this technique, a beam of atoms or ions is directed towards a thin foil, typically constructed of carbon. The beam atoms/ions interact with the carbon atoms, stripping electrons from the moving particles which then recombine to produce a broad range of excitation states that radiatively decay. In earlier configurations of the beam-foil experiment the foil was made to move along the direction of the beam, and a photomultiplier tube at a fixed post-foil location recorded the decay curve. Uncertainties in recording a proper decay curve arise from the need to have a time-independent beam source, highly repeatable mechanical operation of the foil motion, and knowledge of the time-variable characteristics of the foil (thinning and breaking) and Doppler effects, to name a few. The non-selective nature of excitation leads to cascade effects, where higher-lying levels than that being studied can contribute to the population of the level under study if the higher level's lifetime is significantly shorter than that of the level under investigation. Cascading will produce systematically longer lifetimes. This problem was addressed by the introduction of the Arbitrary Normalization Decay Curve (ANDC) correction (Curtis, 1974; and Curtis, Deck & Ellis for a discussion on precision in atomic lifetime measurements), which requires that lifetimes for higher-lying levels also be measured. Lifetimes measured prior to the introduction of the ANDC correction are considered to be more uncertain than quoted. Despite its limitations, the beam-foil approach can be applied to virtually any charge state of any element. The range of lifetimes that can be measured is a function of the beam strength and the distance over which it travels after encountering the foil. An example of an active beam-foil facility is the Toledo Heavy Ion Accelerator (THIA, University of Toledo, Ohio), which is able to record lifetimes in the range 0.5 to 15 ns.

Experiments are generally optimized for work in a specific energy regime, as determined by the ion source. Low energy atomic/ion sources are based on earlier furnace designs to produce a beam of particles in a 1 m long carbon tube heated to 3000 K by high current, which was appropriate for an absorption technique, providing thermal excitation limited to low excitation (3 eV) (Blackwell 1990). Furnaces are still used to produce atomic and ionic beams, although they are now considerably smaller in size (mm to cm length) than earlier models. High-ionization plasmas are now being routinely produced by devices such as the electron-beam ion trap (EBIT) (see Beiersdorfer 2008, 2009 for recent reviews), where an electron beam interacts with magnetically-confined ions.

The shock tube was an earlier technique for measuring oscillator strengths. It could be utilized in either absorption or emission mode, producing LTE conditions over a wide temperature and density range, including stellar atmosphere-like plasma conditions (temperature 3000 to 9000 K and particle density 10^{20} cm^{-3}), but required measurement of plasma temperature and density for analysis. Other laboratory techniques, such as the Hanle effect for lifetime measurement (Hanle 1991) and the hook method for f-values are briefly described by Parkinson (1987). A thorough discussion of the measurement of oscillator strengths up to the mid-1980s is presented by Huber & Sandeman (1986).

3.5 *Example: Oscillator strengths for* Se I

We highlight the discussion of experimental gf-values by considering the available data for Se I.

Like most neutral elements, Se I has a number of published experimental and theoretical studies. The literature contains data for level lifetimes and branching fractions appropriate for determing gf-values for only a few spectral lines, namely, those of multiplets 1, UV1, and UV2. The data in Table 1 represent all Se I

Table 1. gf-values in Se I found in compilations

Wavelength[1] (Å)	log(gf)	E_{low} (eV)	J_{low}	E_{up} (eV)	J_{up}	Labels	Ref[2]
1960.902	−0.23	0.000	2.0	6.323	1.0	$4p^4\ ^3\mathrm{P} - 5s\ ^3\mathrm{S}^o$	CB
2039.851	−0.11	0.247	1.0	6.323	1.0	$4p^4\ ^3\mathrm{P} - 5s\ ^3\mathrm{S}^o$	CB
2062.788	−0.52	0.314	0.0	6.323	1.0	$4p^4\ ^3\mathrm{P} - 5s\ ^3\mathrm{S}^o$	CB
2074.794	−1.44	0.000	2.0	5.974	2.0	$4p^4\ ^3\mathrm{P} - 5s\ ^5\mathrm{S}^o$	CB
2164.165	−1.00	0.247	1.0	5.974	2.0	$4p^4\ ^3\mathrm{P} - 5s\ ^5\mathrm{S}^o$	MULT
8918.803	+1.29	5.974	2.0	7.364	3.0	$5s\ ^5\mathrm{S}^o - 5p\ ^5\mathrm{P}$	CB
9001.898	+0.00	5.974	2.0	7.351	2.0	$5s\ ^5\mathrm{S}^o - 5p\ ^5\mathrm{P}$	GUES
9038.546	+0.00	5.974	2.0	7.345	1.0	$5s\ ^5\mathrm{S}^o - 5p\ ^5\mathrm{P}$	GUES

[1] Vacuum wavelength for $\lambda < 2000$ Å, air wavelength for $\lambda > 2000$ Å.

[2] CB, Corliss & Bozman (1962); MULT, multiplet rules, GUES, guess, (Kurucz 1993)

oscillator strength data that are typically accessed by astronomers. The data were extracted from the Vienna Atomic Line Database (VALD, Kupka et al. 1999), but were compiled by Kurucz (1993) from the CB data.

Atomic lifetime measurements for Se I have been performed with laser techniques by Bengtsson et al. (1992a) for the level $5s\ ^3\mathrm{S}^o{}_1$, 50996.03 cm^{-1} ($\tau =$ 2.9(5) ns, ± 17%) and by Bengtsson et al. (1992b) for the level $5s\ ^5\mathrm{S}^o{}_2$, 48182.19 cm^{-1} ($\tau = 493(15)$ns, ± 3%). Dynefors (1975) measured the lifetime for the levels $5s\ ^1\mathrm{D}_2$ ($\tau = 1.9\pm0.2$ ns), $5s\ ^3\mathrm{S}_1$ ($\tau = 1.7\pm0.2$ ns) and $5s\ ^3P_2$ ($\tau = 2.6\pm0.6$ ns) by the beam-foil technique. Line intensity ratios with estimated uncertainties of 1 to 5 % were published by Ubelis & Berzinsh (1986) ($I_{196.1} : I_{204.0} : I_{206.3} = (100 \pm 1) : (44 \pm 1) : (15 \pm 0.5)$ and $I_{207.5} : I_{216.4} = (100 \pm 5) : (18 \pm 1)$). A history of relative transition probabilities for the lines of Se I multiplet UV2 is presented in Table 2. Although uncertainties have not always been provided for experimental data, it can be seen that theory and experiment have reached agreement to within a few percent. Substituting the intensities from Ubelis & Berzinsch and lifetimes from Bengston et al. into Eqns. 3.2, 3.4 and 3.5 for multiplet UV2 results in the gf-values presented in Table 3. If one assumes the measurement of lifetimes and line intensities to be uncorrelated, then the uncertainty range of 1 to 5% in I, coupled with uncertainty range of 3 to 17% in τ leads to an approximate uncertainty range of 4 to 20% in A and f by application of a least-squares approach (Bevington 1969). A more rigorous approach to error analysis for f-values has been put forward by Sikström et al. (2002). It should be noted that the compilation of resonance line data (Morton 2000) includes gf-values for Se I $\lambda\lambda$1960.902, 2074.794 as given in Table 3. The data for $\lambda\lambda$2039.851, 2062.788, 2164.165 do not appear elsewhere in the literature.

Table 2. Relative transition probabilities for Se I

Reference	$A(196.1)$	$A(204.0)$	$A(206.3)$	Comment
Ubelis & Berzinsh (1986)	100 ± 1	44 ± 1	15.5 ± 0.5	experiment
Garpman et al. (1974)	100	50	17	theory
Gruzdev (1969)	100	48	16	theory
Krempl & Schmid (1968)	100	238	240	experiment
Laurence (1967)	100	47	16	theory
Knox & Olechna (1967)	100	34	3.8	theory
Corliss & Bozman (1962)	100	130	48	experiment

Table 3. Comparison of experimental gf-values for Se I

Wavelength (Å)	log gf CB[1]	log gf (UB + B)[2]	Comment
1960.902	−0.230	−0.426	UV2, resonance line
2039.851	−0.110	−0.747	UV2
2062.788	−0.5	−1.208	UV2
2074.794	−1.440	−2.255	UV1, resonance line
2164.165	−1.000	−2.963	UV1

[1] `CB, Corlis & Bozman (1962)`

[2] BF `from Ubelis & Berzinsh (1986),` τ `from Bengsston et al. (1992a,b)`

4 Oscillator strengths from theory

A strong motivation for constructing large compilations of theoretical f-values is the problem of available resources for conducting costly experiments. Experiments are not undertaken to produce a large number of f-values due to limitations in wavelength coverage, detector sensitivity, techniques to populate excited atomic and ionic states, and the human resources needed to run the experiments. Improvements in computer capabilities and algorithms have lead to the development of sophisticated atomic structure codes, but limitations in run-time for codes still do not allow for running a code for a complete ion.

From the data users' perspective, the utility of atomic structure calculations lies in providing oscillator strengths for a large number of transitions that serve as opacity sources, as well as for specific lines that are used for element abundance analysis. Ultimately, atomic structure models will be able to describe all energy levels, transition probabilities, and scattering parameters (cross-sections for collisions and radiative absorption) to a high degree of accuracy. Experiments are useful for supplying constraints on the calculations, but this comes at the cost of repressing degrees of freedom in *ab initio* calculations.

The theoretical determination of f-values has evolved along with approaches to solving the Schrödinger equation. One defining difference among atomic structure codes is the treatment of relativistic corrections, ranging from non-relativistic (Breit-Pauli or Hartree-Fock) to fully relativistic (multi-configuration Dirac-Fock, MCDHF). The accuracy of calculations for very heavy elements improves by including relativistic corrections, since this approach accounts for electron penetration into the nucleus. Another consideration is the correlation of potentials accounting for different electronic configurations, and the extent of interaction among the electrons, i.e. core-core, core-valence, and valence-valence interactions.

The basic approach to computing oscillator strengths is a multi-step procedure:

1) Wavefunctions are determined and transition energies are computed. At this stage a test can be performed that compares the computed energies with observations, but it is not necessarily done. The wavefunctions can be created with different potentials, techniques and assumptions.

2) The line strength, S, is computed using either the length (r) or velocity (E) operator (O).

$$S(\gamma_i J_i, \gamma_j J_j) = \langle \Psi(\gamma_i J_i) || O || \Psi(\gamma_j J_j) \rangle^2 \tag{4.1}$$

The length form for the calculated line strength is independent of the energy and is more stable to adding new effects. Ideally, $S_{length} = S_{velocity}$ for exact Ψ. For approximate Ψ, this agreement is necessary but not sufficient.

3) The transition probability is then computed from the line strength.

$$A(\gamma_j J_j, \gamma_i J_i) = (4/3)[\alpha \Delta E_{ik}]^3 S(\gamma_i J_i, \gamma_j J_j)/g_j \tag{4.2}$$

4) The oscillator strength is computed from the line strength (or transition probability).

$$f(\gamma_i J_i, \gamma_j J_j) = (2/3)\Delta E_{ik} S(\gamma_i J_i, \gamma_j J_j)/g_i \tag{4.3}$$

Equation 4.3 can be compared with formulae linking A, f, and S (e.g. Wiese & Martin 1980).

$$g_i f_{ij} = 1.499 \times 10^{-8} \lambda^2 g_j A_{ji} = 303.8 \lambda^{-1} S, \tag{4.4}$$

where the units are $\lambda(\mathring{A})$, $A(10^8\ \mathrm{s}^{-1})$, and S in atomic units.

Uncertainties for computed f-values do not carry the same meaning as uncertainties from experiments. The theoretical uncertainty can be coupled to experimental uncertainties for semi-empirical approaches that use the experimental energy levels as constraints. However, theoretical uncertainties are normally associated with tests that are performed for computational convergence and the prediction of the energy level system compared with those determined from experiment. Transition energies, ΔE, are used as tests of *ab initio* calculations. This is not appropriate for semi-empirical calculations (Cowan code (1981), for example), where the energies are fixed as input.

The agreement between the *length* and *velocity* f-values is a second test. It is a more reliable test for the case of LS-coupling with non-relativistic theory. The velocity form in relativistic theory is more difficult to work with since it is transition dependent.

As a final note on theoretical uncertainties, there seems to be as many research groups as there are versions of codes and one must be careful to understand the different conditions of their analyses and whether these conditions are suitable for the transitions that the data user will study. Consulting the atomic data producer is always good practice, whether the data are experimental or theoretical. The reader is referred to Butler (this volume) for discussions on certain theoretically determined atomic data, and to the work of Froesh-Fischer (2009) for a discussion on error analysis for theoretically derived transition data.

5 Comments on astrophysical gf-values

For many spectral lines both experiment and theory have not provided a gf-value of reasonable uncertainty. This is often the case when experimental data pertaining to the line's branching fraction or lifetime is unknown, and as mentioned above, theoretically derived gf-values may have large or indeterminable uncertainties. Determining atomic data directly from the source spectrum under investigation can provide useful information. When the source spectrum is that of an astronomical object the atomic data (wavelengths, gf-values, line broadening constants, etc.) derived from it are referred to as an astrophysical quantity; for example, an astrophysical gf-value.

The majority of astrophysical gf-values are derived from observations of solar absorption lines (c.f. Meléndez & Barbuy, 1999; Thévenin, 1990), where LTE conditions might be assumed, or from resonance lines originating from the interstellar medium (Cardelli & Savage 1995). The element abundance must be known from an independent determination, such as from spectral lines whose atomic data are known to high accuracy. The astrophysical gf-value is then determined through either the application of Eq. 1.1 for a measured equivalent width or by adjusting the gf-value in a synthetic spectrum fit to the observed spectral line while keeping the element abundance fixed. Since the astrophysical gf-value is determined from a specific stellar spectrum, it is most useful when:

- studying stars of similar spectral type, luminosity class and metallicity, thereby leading to a relative abundance analysis among similar type stars
- the spectral line serves in the capacity of background opacity or line blending
- the spectral line serves to confirm an abundance.

Even under the best of circumstances, astrophysical gf-values serve only as estimates to accurate experimental gf-values. The uncertainties in astrophysical gf-values can be very large, and this uncertainty is transferred directly to the uncertainty in the element abundance determined from that line, since the abundance is inversely proportional to the gf-value for a line's equivalent width (Eq. 1.1). The sources of uncertainty in the derivation of an astrophysical gf-value are many, and we list some of the more obvious concerns of the analysis.

- If the spectral type of the star determining the gf-value is not the same as the stars for which it will be used, then different excitation and line blending conditions would exist.

- If the ion that is being used to determine an astrophysical gf-value is not the same as that used for determining the abundance of the element, then different conditions (excitation, ionization, non-LTE) among stars may lead to higher uncertainty.
- The uncertainty of the astrophysical gf-value includes the uncertainties of lines used to determine the element abundance. Uncertainties are introduced by the method of determining the abundance that will be used to derive the astrophysical gf-value (line blending, continuum placement, line fitting or measurement of equivalent width).
- The astrophysical gf-value is associated with the specific spectrum used to determine it (S/N, resolution, data reduction technique).
- Improperly treated line structure, including hyperfine structure, isotope shift and magnetic line structure, and can affect the abundance determined from lines having known gf-value, as well as the derived astrophysical gf-value.
- The astrophysical gf-value is associated with the code used for data analysis, its explicit assumptions in calculating equivalent widths or line profiles, the analytical expressions and default values (ionization potential, partition functions). The analysis is platform dependent.
- Astrophysical gf-values can be determined when the abundance of an element is not determined from the stellar spectrum but is assumed to be that of the chondritic meteorite value. Meteoritic element abundances have their own uncertainties, which should be cautiously interpreted.

Unfortunately, when it is assumed that all spectral lines of a species would yield the same element abundance, astrophysical gf-values would not be useful in a non-LTE analysis, other than to describe line blending, since a non-LTE approach computes line strength based on variable level populations as a function of atmospheric depth. Any of the above listed concerns may amount to a small effect, but the presence of several of them may enter into the astrophysical gf-value and its uncertainty in intractable ways.

6 f-values and line structure

Essentially all elements will produce complex line profiles when their spectra are viewed at sufficiently high spectral resolution and under conditions of weak line broadening (Doppler, collisional). Most elements have multiple stable isotopes, and many of these isotopes have an odd number of nucleons, which introduces hyperfine structure (HFS) into the spectral line profile. It is only for thorium, which possesses only a single, even-numbered stable isotope, that we would not expect to observe line structure. Fortunately, the BF and τ parameters of the experimental gf-value can be measured using lower spectral resolution than that needed to detect line structure, and no isotope separation techniques are required.

Here, we consider only line structure in the form of isotope shift (IS) and hyperfine splitting of the energy levels, neglecting the effects of external magnetic fields leading to, for example, the Zeeman effect. Isotope shift results from the nuclear mass and charge distributions shifting atomic energy levels. Three forms of IS are considered: 1) normal mass shift, 2) volume (or field) shift, and 3) specific mass shift. For the light elements, lighter than the iron group, the addition of a single neutron is sufficient to change the electron orbits according to the normal mass shift via a reduced mass effect that shifts the electronic states, leading to a frequency shift of a spectral transition for different isotopes. The transition probability remains the same transition for the different isotopes. For the heaviest elements, the addition of a neutron does not have a noticeable effect on the valence electron orbits due to screening effects. However, the additional nucleon alters the charge distribution of the nucleus, and core-penetrating electron orbits will be affected more than non-penetrating orbits. Frequency shifts can result among different isotopes for transition states that are disproportionately affected. For elements intermediate to these regimes, both the normal mass and volume shifts are not particularly large, but the spectral line can be shifted according to the specific mass shift, which must be calculated to understand its influence contribution. The specific mass shift is the expectation value of an operator involving electron momenta (see Froese Fischer & Smentek-Mielczarek (1983) for an explanation of the specific mass shift).

Hyperfine structure of energy levels is the result of the mutual interaction of the electric fields originating from the nucleus and the electrons. The number of components making up the HFS pattern is governed by the quantum numbers S, L, and I. Each fine structure level involved in the transition is split into a number of hyperfine levels given by the smaller of the two numbers $2J$ +1 or $2I + 1$. The number of HFS components of the transition is governed by the usual selection rules. Ignoring the case of no HFS ($J_i = 0 <-> J_j = 0$), the number of HFS components of an isotope typically range from 2 ($I = 1/2$) to 16 (when $J = 15/2$).

The effects of HFS and IS are often simultaneously present in a spectral line. For lines on the linear portion of the curve of growth the presence of obvious line structure will reduce the peak intensity and broaden a spectral feature when observed at the spectral resolution of astronomical spectrographs, which are typically lower than the laboratory spectrographs used to analyze line structure. If the hyperfine components have a large range in oscillator strength, then line saturation effects will act differently among them. The weaker components may not be contributing to the line profile, which will induce an error equivalent to the portion of the line total f-value that is not detected (Wahlgren 2005).

Line broadening by IS and HFS is dependent on the electron orbitals of the transition. For heavy elements, the deeper penetration of the s orbital into the nucleus belies its higher eccentricity than other orbitals. A transition involving s orbitals for both lower and upper states, i.e. where the transition represents a change from/to an s orbital, or from/to a ns^2 to $ns\ ml$ where l is not equal to s, would be expected to have a greater IS and HFS than a transition between higher orbitals, for example, transitions between the d and f orbitals.

Table 4. Line structure for Tl II λ1908[1]

Isotope Mass Number	F_l	F_u	Wavelength Å	gf (stat.wt.ratio)	gf (terrestrial)
203	0.5	1.5	1908.5632	0.030	0.0088572
	0.5	0.5	1908.6982	0.015	0.0044286
205	0.5	1.5	1908.5725	0.030	0.0211428
	0.5	0.5	1908.7087	0.015	0.0105714

[1] Based on Johansson et al. (1996)

Including the combined effects of HFS and IS, the f-value for spectral transition component i for one of the atom's isotopes can be written as

$$f_i = f_{total} \frac{A_{el/isotope}}{A_{el}} (BF)_{HFS,i} \,, \tag{6.1}$$

where f_{total} is the total f-value for the transition, the ratio of $A_{el/isotope}$ to A_{el} is the fraction of an element in a specific isotope, and $(BF)_{HFS,i}$ is the branching fraction of component i in the HFS pattern.

As an application of Eq. 6.1, we deconvolve the total gf-value of the resonance line $6s^2$ ^{1}S$_0$ - $6s6p$ ^{3}P$_1{}^o$ Tl II λ1908 into the gf-values for its isotope and hyperfine components. Terrestrial thallium is comprised of two stable isotopes of relative contribution ^{203}Tl:^{205}Tl = 0.29524:0.70476 (IUPAC 1998). Since each isotope has an odd-number of nucleons the spectral transition for each isotope will possess HFS. According to the selection rules of LS-coupling, the transition will be comprised of four components, two hyperfine components for each isotope. From theory the total gf-value of the transition is $gf = 0.045$ (Johansson et al. 1996). Each isotope of this transition will have this gf-value, since the transition probability is independent of isotope. For each isotope, the hyperfine component gf-values can be obtained by: a) measurement of relative intensities of hyperfine components from high-resolution laboratory spectra, b) general relationships derived using 6-j symbols, or c) application of sum rules. From each of these methods the ratio of gf-values for the hyperfine components for each isotope of this Tl II transition is 2:1. Table 4 presents the gf-values for each of the four components of this transition.

When inserting gf-value data for line structure into programs that generate synthetic spectra, one must be aware of whether the code accounts for the relative isotope composition assumed for the stellar atmosphere. If the program does not accept the relative isotope abundances as an explicit input, then the gf-values must be adjusted for each component to account for the relative isotopic abundances, according to Eq 6.1. For the terrestrial (solar system, chrondritic) isotope mixture in our example, the gf-value is multiplied by the relative abundance of the appropriate thallium isotope given above, resulting in the values presented in the right-hand column of Table 4.

7 Concluding remarks

The purpose of this discussion has been to put forward considerations of the uncertainties of oscillator strengths, from which it can be determined whether non-LTE analyses will be particularly susceptible to misinterpretation. We have mentioned sources of uncertainty without providing specifics on their values because of the dependence on many factors, including instrumentation and experiment design, data quality and analysis, and even human nature. Uncertainty designations were established at the National Bureau of Standards (NBS, Washington DC, now the National Institute of Standards and Technology, NIST). The uncertainties are generally assigned according to the standards and techniques employed. Uncertainties have the letter designations: AA $< 1\%$, A $< 3\%$, B $< 10\%$, C $< 25\%$, D $< 50\%$, E $> 50\%$. The majority of available measured gf-values have an accuracy no better than C, although recent experiments often attach uncertainities equivalent to the B designation, or better. For *ab initio* calculations of f-values the uncertainty is not considered in the same manner as experiment uncertainties. Theoretical gf-values may not have uncertainties designated by the authors, and when assigned by others, the uncertainty tends to be the equivalent of the E label. This can give a misleading impression of theoretical work, since highly accurate results can be produced, especially for the lightest elements and one-electron systems.

The uncertainty of the gf-values must be carefully considered when using a mixture of data sources. A particular consideration is whether one should mix sources of data having very different degrees of uncertainty. One must balance the importance of whether to use relatively few lines for an abundance analysis if they originate from a single study with low uncertainties versus using many lines from multiple sources in an effort to reduce systematic errors. Modern experiments for f-values may have systematics, but they seem to be a lower level than the uncertainty introduced from using multiple sources. For extensive non-LTE analyses, it may be necessary to use multiple data sources, including calculations for high excitation transitions. But in general, the most egregious f-values should not be included into the data analysis, as they will only serve to increase the uncertainty of the result and may introduce systematics. When using relatively few lines in an analysis, culling the line list for poor f-values should be considered. A line with a very high uncertainty may have worse consequences for the science than not using the line.

As a final word of caution regarding uncertainties, one should be suspicious that they are underestimated. We do not fully understand the intricate interactions among photons and matter. Also, our understanding of the laboratory experiments and atomic structure theory is not complete.

The author would like to thank Lars Engström (Lund University) for making available the figure for the Tl III lifetime measurement, and Gill Nave (NIST) for help with laboratory experiments with selenium. This work has been carried out with funding from NASA grant NNG06GJ29G.

References

Bashkin, S., 1964, Nucl. Instr. and Meth., 28, 88

Beiersdorfer, R., 2008, Can. J. Phys., 86, 1

Beiersdorfer, R., 2009, Phys. Scripta, T134, 014010

Bengtsson, G.J., Berzinsh, U., Larsson, J. & Svanberg, S., 1992a, Z. Phys. D, 23, 29

Bengtsson, G.J., Berzinsh, U., Larsson, J., Svanberg, S. & Zerne, R., 1992b, J. Phys. II France 2, 773

Bevington, P.R., 1969, Data Reduction and Error Analysis for the Physical Sciences, (McGraw-Hill: New York)

Blackwell, D.E., 1990, in Atomic Spectra and Oscillator Strengths for Astrophysics and Fusion Research (ASOS3 proceedings), ed. J E Hansen, (North-Holland : Amsterdam), p.160

Blackwell, D.E. & Collins, B.S., 1972, MNRAS, 157, 255

Bord, D.J., Barisciano, L.P. & Cowley, C.R., 1996, MNRAS, 278, 997

Cardelli, J.A. & Savage, B.D., 1995, ApJ, 452, 275

Corliss, C.H. & Bozman, W.E., 1962, Experimental Transition Probabilities for Spectral Lines of Seventy Elements, NBS monograph 53

Cowan, R.D., 1981, The Theory of Atomic Structure and Spectra, (Univ. of California Press : Berkeley)

Cowley, C.R., 1983, MNRAS, 202, 417

Cowley, C.R. & Corliss, C.H., 1983, MNRAS, 203, 651

Cowley, C.R. & Warner, B., 1967, The Observatory, 87, 117

Curtis, L.J., 1974, JOSA, 64, 495

Curtis, L.J., Deck, R.T. & Ellis, D.G., 1997, Physics Letters A, 230, 330

Ditchburn, R.W., 1963, Light, 2nd edition, Blackie & Son Limited, (London : UK)

Dynefors, B.I., 1975, Phys. Scripta, 11, 375

Froese Fischer, C., 2009, Phys. Scripta, T134, 014019

Froese Fischer, C. & Smentek-Mielczarek, L., 1983, J. Phys. B, 16, 3479

Fivet, V. et al., 2008, J. Phys. B, 41, 015702

Garpman, S., Holmgren, L. & Rosen, A., 1974, Phys. Scripta, 10, 221

Garstang, R.H., 1968, *Atomic Transition Probabilities*, in Beam-Foil Spectroscopy, Vol II, ed. S. Bashkin, (Gordon & Breach Science Publishers : New York)

Gruzdev, P.F., 1969, Opt. Spectr., 27, 479

Hanle, W., 1991, Z. Phys. D, 18, 3

Huber, M.C.E. & Sandeman, R.T., 1986, Rep. Prog. Phys., 49, 397

IUPAC, International Union of Pure and Applied Chemistry 1998, *Isotopic Compositions of the Elements, 1989* in Pure and Applied Chemistry, 70, 217

Johansson, S., Kalus, G., Brage, T., Leckrone, D.S. & Wahlgren, G.M., 1996, ApJ, 462, 943

Kay, L., 1963, Phys. Letters, 5, 36

Knox, R.S. & Olechna, D.J., 1967, J. Chem. Phys., 47, 5226

Krempl, H. & Schmid, G., 1968, Spectrochimica Acta, 23B, 819

Kupka, F., Piskunov, N., Ryabchikova, T.A., Stempels, H.C. & Weiss, W.W., 1999, A&AS, 138, 119

Kurucz, R., 1993, CD-ROM18, cfa-www.harvard.edu/amp/ampdata/Kurucz218/sekur.html

Ladenburg, R., 1921, Z. für Physik, 4, 451

Ladenburg, R., 1928, Z. für Physik, 48, 15

Ladenburg, R., 1933, Rev. Modern Physics, 5, 243

Laurence, G.M., 1967, ApJ, 148, 261

Li, Z.S., Lundberg, H., Sikström, C.M. & Johansson, S., 1999, Eur. Phys. J., D6, 9

Mannervik, S., 2003, Phys. Scripta, T105, 67

Martinson, I., 1998, Proceedings of the International School of Physics "Enrico Fermi", Course CXXXVII, eds. I. Bigi & L. Moroni, (IOS Press : Amsterdam), pp. 625-636

Meggers, W.F., Corliss, C.H. & Scribner, B.F., 1975, NBS Monograph 145, (US Govt Printing Office : Washington DC)

Meléndez, J. & Barbuy, B., 1999, ApJ, 124, 527

Mihalas, D., 1978, Stellar Atmospheres, 2nd edition, (W.H. Freeman and Company : San Francisco)

Morton, D., 2000, ApJS, 130, 403

Parkinson, W.H., 1971, in Shock Tube Research, Proceedings of the Eighth International Shock Tube Symposium, eds. J.L. Stollery, A.G. Gaydon, A. & P.R. Owen, (Chapman and Hall: London)

Parkinson, W.H., 1987, in Spectroscopy of Astrophysical Plasmas, eds. A. Dalgarno & D. Layzer, (Cambridge Univ. Press: Cambridge)

Sikström, C.M., Litzén, U., Blom, A. & Lundberg, H., 2002, JQRST, 74, 355

Thévenin, F., 1990, A&AS, 82, 179

Thorne, A., Litzén, U. & Johansson, S., 1999, Spectrophysics, (Springer-Verlag: Berlin)

Ubelis, A. & Berzinsh, U., 1986, Phys. Scripta, 34, 805

Wahlgren, G.M., Brage, T., Brandt, J. C. et al, 2001, ApJ, 551, 520

Wahlgren, G.M., 2005, Mem. Soc. Astron. Italia Suppl., 8, 108

Wiese, W.L. & Martin, G.A., 1980, Wavelengths and Transition Probabilities for Atoms and Atomic Ions, Part II. Transition Probabilities, NSRDS–NBS68, (US Govt Printing Office : Washington DC)

Zwaan, C., 1967, Bull. Astr. Inst. Netherlands, 19, 1